PERFORMANCE OF GRAPHENE OXIDE AND COCONUT SHELL ACTIVATED CARBON FOR ^{131}I ISOLATION FROM DELAY TANK

FARA HANA BINTI MOHD HADZUAN

UNIVERSITI SAINS MALAYSIA

2023

PERFORMANCE OF GRAPHENE OXIDE AND COCONUT SHELL ACTIVATED CARBON FOR ^{131}I ISOLATION FROM DELAY TANK

by

FARA HANA BINTI MOHD HADZUAN

Thesis submitted in fulfilment of the requirements

for the degree of

Master of Science

July 2023

ACKNOWLEDGEMENT

All praises to Allah SWT for the protection and ability to accomplish this MSc journey. I would like to acknowledge and give my warmest thanks to my main supervisor, Dr Mohammad Khairul Azhar bin Abdul Razab for the guidance, continuous support and help from the beginning of planning and constructing of experiment that had carried me through all the stages of finishing this project. I would also like to give special thanks to two of my co-supervisors, Dr Norazlina binti Mat Nawi and Prof. Madya Ts. Dr Nor Hakimin bin Abdullah for their opinions and generously sharing their knowledge with me. I'm also thanking USM for granting me the opportunity for being part of postgraduate society also for sponsoring me with GRA-assist sponsorship. This work was supported by a Short-Term Research Grant from Universiti Sains Malaysia [304/PPSK/6315499]. Also, thanks to all the laboratory staff in PPSK who were not weary to help and guide me.

Special thanks to my family especially my grandparents, MD. Saad bin Othman and Halijah binti Harun for believing and supporting in every decision that I made, also their continuous encouragement, prayers and love had made me who I am today. My sincere indebtedness and gratitude to my fellow friends Rosidah binti Sunaiwi and Nur Atiqah Syahirah binti Shari for their constant kindness and help especially during the experiment execution. I am also immensely thankful to my partner, Muhammad Nabil for the unwavering support and assurance, thank you for tagging along in this rollercoaster journey, always. Last but not least, I want to thank me for believing in me, I want to thank me for never quitting and for doing all this to reach for the stars.

Fara Hana Binti Mohd Hadzuan
August 2022

TABLE OF CONTENTS

ACKNOWLEDGEMENT ..... **ii**

TABLE OF CONTENTS ..... **iii**

LIST OF TABLES ..... **ix**

LIST OF FIGURES ..... **x**

LIST OF EQUATIONS ..... **xv**

LIST OF ABBREVIATIONS ..... **xvi**

LIST OF APPENDICES ..... **xvii**

ABSTRAK ..... **xviii**

ABSTRACT ..... **xx**

CHAPTER 1 INTRODUCTION **1**

1.1 Background of Study 1

1.2 Problem Statement 3

1.3 Study Objectives 4

1.3.1 General Objectives 4

1.3.2 Specific Objectives 5

1.4 Study Significant 5

1.5 Conceptual Framework 6

CHAPTER 2 LITERATURE REVIEW 7

2.1 Radioiodine Therapy 7

2.1.1 Decay Rate of ^{131}I Radionuclide 9

2.2 Clinical Radioactive Waste Management and Delay Tank 11

2.2.1 Radioiodine Therapy and Delay Tank Operation at Nuclear Medicine Department, HUSM 13

2.2.2 Radiation Protection Principles in Malaysia 14

2.3 Carbon-Based Materials 17

2.3.1 Graphene Oxide 17

2.3.2 Coconut Shell Activated Carbon 21

2.4 Adsorption Mechanisms in Aqueous Solution 24

2.5 Morphological Study via FESEM 27

2.5.1 FESEM Studies on Carbon-Based Materials 28

2.6 Crystallinity Study via XRD 30

2.6.1 XRD Studies on Carbon-Based Materials 31

2.7 Composition Studies via XPS 33

2.7.1 XPS Studies on Carbon-based Materials 35

2.8 Absorbability Study via UV-Vis Spectrophotometry 36

CHAPTER 3 METHODOLOGY 38

3.1 Study Design 38

3.2 Study Variables 38

3.2.1 Type of Carbon-Based Materials 38

3.2.2 Concentration of Each Carbon-Based Materials 38

3.2.3 Decay Rate of ^{131}I Radioactive Wastewater 39

3.3 Materials 39

3.3.1 Graphite 39

3.3.2 Coconut Shell Husk 40

3.3.3 ^{131}I Clinical Wastewater 41

3.3.4 Chemicals 42

3.3.5 Apparatus 44

3.4 Scientific Instrument and Analysis Equipment 45

3.4.1 pH Meter 45

3.4.2 Magnetic Stirrer 46

3.4.3 Furnace 47

3.4.4 Centrifuge 47

3.4.5 Dose Calibrator 48

3.4.6 Geiger-Müller Counter 49

3.4.7 Pen Dosimeter 50

3.4.8 FESEM and EDX 51

3.4.9 UV-Vis Spectrometer 52

3.4.10 XRD 52

3.4.11 XPS 53

3.5 Methods 55

3.5.1 Carbon-Based Materials Preparation 56

3.5.1(a) Synthesis of GO via Hummers Method 56

3.5.1(b) Synthesis of CSAC 58

3.5.1(c) Determining the Carbon-Based Materials Concentrations 61

3.5.1(d) Carbon-Based Materials Concentration Preparation 62

3.5.2 Extraction of ^{131}I from Clinical Waste Water 64

3.6 Data Analysis 67

3.6.1 Kinetic Radioactivity Study 67

3.6.2 Radioactive Sediment Characterization 69

3.6.2(a) Morphology Study via FESEM 69

3.6.2(b) Crystallinity Study via XRD 72

3.6.2(c) Binding Energy Determination via XPS 76

3.6.3 Absorbability Study via UV-Vis Spectrometer 77

3.7 Waste Disposal After Experimental Procedures 79

CHAPTER 4 RESULT AND DISCUSSION 80

4.1 Kinetic Study of the Extracted ^{131}I from Clinical Wastewater 80

4.2 Characterization Study of Synthesized Carbon-Based Materials and Extracted ^{131}I Radionuclide from Wastewater 86

4.2.1 Morphological Study via FESEM 86

4.2.1(a) Pure GO and Extracted ^{131}I Morphology 87

4.2.1(b) Pure CSAC and Extracted ^{131}I Morphology 91

4.2.2 Crystallinity Study 95

4.2.3 Composition Study 99

4.3 Absorbability Study on Carbon-Based Materials and Extracted ^{131}I 103

4.4 Adsorbability Mechanism Study 106

CHAPTER 5 CONCLUSION 110

5.1 Conclusion 110

5.2 Recommendations for Future Study.....111

REFERENCES.....114

APPENDICES

LIST OF PUBLICATION

LIST OF TABLES

Page

Table 2.1 Classification of working areas 16

Table 2.2 Applications of GO as an adsorbent of heavy metals in wastewater 18

Table 2.3 Comparison of BET specific surface area and average pore diameter from previous studies on different types of Activated Carbon 23

Table 2.4 2-Theta and d-spacing values based on various GO-based samples via XRD analysis 32

Table 2.5 2-Theta and d-spacing values based on CSAC and other molecules adsorption via XRD analysis 33

Table 3.1 List of chemicals used in Graphene Oxide and Coconut Shell Activated Carbon preparation 42

Table 3.1 Continued..... 43

Table 3.2 The variation of GO concentrations mg/ml..... 62

Table 3.3 The variation of CSAC concentrations mg/ml 63

Table 3.4 Measurement of radioactivity for ^{131}I according to the natural decay time 67

Table 4.1 R^2 values obtained for different concentrations of GO:^{131}I and CSAC:^{131}I..... 82

Table 4.2 XRD result obtained based on the 4 types of sample..... 96

Table 4.3 XPS result and the bonds indication of GO and GO:^{131}I 101

Table 4.4 XPS results and bonds indication of CSAC and CSAC: ^{131}I..... 103

LIST OF FIGURES

Page

Figure 1.1 Conceptual framework of this research 6

Figure 2.1 The ^{131}I uptake mechanism by the thyroid gland 9

Figure 2.2 The radioactive decay of ^{131}I via betta emission obtaining a stable ^{131}Xenon and gamma radiation. 10

Figure 2.3 The plan of a measurement point at the ^{131}I delay tank room at the Nuclear Medicine department, HUSM 13

Figure 2.4 Bar chart represents the number of patients for each radioiodine therapy and diagnostic scan 14

Figure 2.5 Graphene oxide honey-comb structure with various oxygen-containing functional groups 19

Figure 2.6 Different types of pores on activated carbon 22

Figure 2.7 The adsorption mechanism of GO towards heavy metals where the heavy metals ion interact with the oxygen-contained functional groups on the surface of GO nanosheets 25

Figure 2.8 CPS adsorption on CSAC 26

Figure 2.9 Illustration of main components of SEM (Mokobi, 2022) 27

Figure 2.10 Agglomeration between GO and ^{131}I image obtained via FESEM 29

Figure 2.11 SEM image obtained from a selected micrometre area of synthesized CSAC 30

Figure 2.12 Determining the CrI based on the peak area, total area and Y-axis baseline 32

Figure 2.13 Different transitions between the bonding and anti-bonding electronic states where light energy is absorbed in UV-Vis spectrophotometry 36

Figure 3.1 Graphite 40

Figure 3.2 Raw coconut shell husk 40

Figure 3.3 The collected wastewater in centrifuge bottle kept in lead shield transporter 41

Figure 3.4 (a) PTFE membrane filter was used to filtrate the sediment of ^{131}I waste water;(b) Two 10 mL crucibles were filled with coconut shell mixture that was heated in the furnace 44

Figure 3.5 Size comparison of 15 mL and 50 mL centrifuge bottles that were used in the centrifuge process for both GO and CSAC. They were also used in the extraction of ^{131}I from radioactive waste water 45

Figure 3.6 (Eutech Benchtop pH700) pH meter used to measure the pH level of prepared carbon-based materials 46

Figure 3.7 (a) The stirring hot plate, will continuously stir the mixture with the (b) stationary electromagnet immersed in the solution 46

Figure 3.8 Carbolite furnace, model CWF 1300 used in this study 47

Figure 3.9 (a) Universal 32 R Centrifuge machine, model CTF15-002 was used along with 50 mL centrifuge bottles (b) to separate the fluid components. 48

Figure 3.10 (a) The ATOMLAB 500 dose calibrator reading screen and also function as the equipment setting platform are connected to the ionization chamber (b) that will hold and measure the radioactive material 49

Figure 3.11 The SE International Inspector brand GM counter was used in the delay tank room to ensure the radiation exposure was within the safety limit 50

Figure 3.12 Pen Dosimeter, Model MyDose mini, S/N 16822 provided by Nuclear Medicine Department, HUSM 51

Figure 3.13 FESEM, Model FEI QuantaTM 450 FEG 51

Figure 3.14 UV-Visible Spectrometer, Model Cary 100 52

Figure 3.15 XRD machine model D8 Advance was used to observe the sediments of carbon-based materials and the ^{131}I located at USM, main campus 53

Figure 3.16 XPS machine model Kratos Axis Ultra DLD located at i-CRIM Research Centre, UKM 54

Figure 3.17 shows the summary of the methodology of this study 55

Figure 3.18 The summary of GO synthesis 57

Figure 3.19 The continuation of GO synthesis summary 58

Figure 3.20 Coconut shell husks were purchased from a local market 59

Figure 3.21 Summary of CSAC synthesis 60

Figure 3.22 (a) A plain filter paper weighed (b) 1 mL of adsorbent dropped on top of the filter paper and weighed 61

Figure 3.23 Varying the GO concentration into small glass bottles 63

Figure 3.24 CSAC solution diluted according to the specific concentrations 64

Figure 3.25 The extraction was done behind a ”L” block radiation shield 65

Figure 3.26 Summary of extraction of ^{131}I from wastewater 66

Figure 3.27 (a) The dose calibrator monitor to s how the radioactivity reading (b) Cylindrical well ionization chamber that holds the radionuclide 67

Figure 3.28 One of the centrifuge bottle containing the sediment, filter paper and filtrate were measured with dose calibrator 69

Figure 3.29 Table-top sputter coater model LEICA EM SCD005 used to coat the samples with gold 70

Figure 3.30 The samples before (a) and after being gold coated (b) to be analyzed via FESEM 70

Figure 3.31 The gold coated samples were placed on top of the sample holder and beamed on with specific parameters 71

Figure 3.32 The sample in powder form was placed on the PMMA Quartz sample holder before being pressed flatly to cover all the sample holder surface 73

Figure 3.33 The sample holders were occupied with different types of samples ... 74

Figure 3.34 CSAC XRD plotted graph that been referred in order to obtain the CrI value 75

Figure 3.35 Distilled water, diluted CSAC, diluted CSAC:^{131}I, diluted GO, diluted GO: ^{131}I, and undiluted GO been distributed in the cell with the labels a, b, c, d, e, and f respectively 78

Figure 3.36 Multi-cell holder occupied for UV-Vis spectrometry analysis 79

Figure 4.1 The plotted graph of ^{131}I activities and GO 81

Figure 4.2 The plotted graph of ^{131}I activities and CSAC 82

Figure 4.3 Bar graph presenting the decay rate acceleration percentage differences of GO and CSAC mixture with five different concentrations from the control sample 84

Figure 4.4 FESEM image of pure GO sample at magnification 15,000x of 10 μm 88

Figure 4.5 FESEM image of pure GO sample at magnification 100,000x of 1 μm 89

Figure 4.6 FESEM image of pure GO sample at magnification 100, 000x of 1 μm 89

Figure 4.7 FESEM image of extracted ^{131}I from wastewater by GO at magnification 5,000x of 10 μm 90

Figure 4.8 FESEM image of extracted ^{131}I from wastewater by GO at magnification 1,000x of 50 μm 91

Figure 4.9 FESEM image of pure CSAC sample at magnification 10,000x of 5 μm 92

Figure 4.10 FESEM image of pure CSAC sample at magnification 20,000x of 4 μm 93

Figure 4.11 FESEM image of extracted ^{131}I from wastewater by CSAC at magnification 10,000x of 5 μm (pore front-view) 94

Figure 4.12 FESEM image of extracted ^{131}I from wastewater by CSAC at magnification 10,000x of 5 μm (pore side-view) 94

Figure 4.13 XRD pattern of GO and GO:^{131}I indicating the peaks 97

Figure 4.14 XRD pattern of CSAC and CSAC:^{131}I indicating the peaks 98

Figure 4.15 Bonds existence identified based on C1s spectra of XPS analysis on GO sample 100

Figure 4.16 Bonds existence identified based on C1s spectra of XPS analysis on GO:^{131}I sample 101

Figure 4.17 Bonds existence identified based on the C1s spectra of XPS analysis on CSAC sample 102

Figure 4.18 Bonds existence identified based on the C1s spectra of XPS analysis on CSAC: ^{131}I sample 103

Figure 4.19 The light absorbed at a certain wavelength (nm) by GO and GO: ^{131}I 105

Figure 4.20 The light absorbed at certain wavelength (nm) by CSAC and CSAC:^{131}I 106

Figure 4.21 Interactions occurred on graphene oxide's sheet 107

Figure 4.22 ^{131}I clinical wastewater interaction with CSAC 109

LIST OF EQUATIONS

$A = \lambda N$	(Eq 1)	10
$n\lambda = 2d \sin\theta$	(Eq 2)	31
Crystallinity Index (CrI)	(Eq 3)	32
$E_k = hv - E_b - \Phi$	(Eq 4)	34
Weight of 1 mL adsorbent	(Eq 5)	61
Adsorbent concentration (mg/mL)	(Eq 6)	61
$M_1V_1 = M_2V_2$	(Eq 7)	62
$\ln (A/A_o) = \lambda t$	(Eq 8)	68
Decay rate acceleration percentage difference	(Eq 9)	83

LIST OF ABBREVIATIONS

GO	Graphene Oxide
CSAC	Coconut shell activated carbon
CrI	Crystallinity Index
^{131}I	Iodine-131
RAI	Radioactive Iodine
FESEM	Field Emission Scanning Electron Microscope
XRD	X-ray Diffraction
XPS	X-ray Photoelectron Spectroscopy
UV-Vis	Ultra Violet-Visible
KBq	Kilobecquerel
HUSM	Hospital Universiti Sains Malaysia

LIST OF APPENDICES

Appendix A Tables of data measurements of extracted ^{131}I from delay tank via GO and CSAC with varied concentrations

Appendix B FESEM images of pure GO and GO:^{131}I

Appendix C FESEM images of CSAC and CSAS:^{131}I

Appendix D The periodical clearance of delay tank at Nuclear Medicine Department, HUSM is on the fifth month (fourth week)

Appendix E Crystallinity Index (CrI) percentage calculation for GO, GO:^{131}I and CSAC:^{131}I

PRESTASI GRAFIN OKSIDA DAN TEMPURUNG KELAPA YANG TELAH DIKARBON AKTIFKAN BAGI ISOLASI ^{131}I DARI TANGKI TANGGUH

ABSTRAK

Iodin-131 merupakan radionuklida yang mempunyai 8 hari separuh hayat dan 971 keV tenaga lebihan. Ciri-ciri ini membuatkan ia sering digunakan bagi rawatan hipertiroidsme dan kanser tiroid. Memandangkan ia mempunyai separuh hayat yang diklasifikasikan rendah-sederhana, pesakit tiroid kanser berbeza (DTC) diberikan ^{131}I yang mempunyai tenaga yang tinggi dan perlu diisolasi sehingga mencapai pendedahan dos sinaran yang minima. Sistem bawah tanah yang dikenali sebagai tangki tangguh digunakan bagi menyimpan sisa ^{131}I dan air kumbahan klinikal sehingga tahap tidak berbahaya dicapai, sebelum dilepaskan ke sistem kumbahan utama. Jabatan Perubatan Nuklear, HUSM, hanya mempunyai dua wad isolasi bagi pesakit DTC dan setiap tangki tangguh mempunyai had kapasiti yang secara langsung mengehadkan jumlah pesakit untuk mendapatkan rawatan tersebut. Oleh itu, teknik alternatif menggunakan grafin oksida (GO) dan tempurung kelapa yang telah dikarbon aktifkan (CSAC) dicadangkan bagi pemencilan sisa kumbahan ^{131}I daripada tangki tangguh. Konsentrasi GO dan CSAC dipelbagaikan lalu dicampur dengan sisa kumbahan radioaktif dan ditapis menggunakan kertas penapis membran bagi mengumpul mendapan. Kadar pereputan konsentrasi 5 mg/mL kedua-dua bahan karbon didapati lebih tinggi berbanding konsentrasi 1, 2, 3, dan 4 mg/mL; ini menunjukkan interaksi aktif telah berlaku. Bahan karbon yang dihasilkan serta mendapan terkumpul telah dianalisa dalam beberapa kajian pencirian; imbasan mikroskopi electron pancaran medan (FESEM) mendapati bahawa GO dan CSAC kelihatan seperti kedutan tisu dan terdapat mikropori pada permukaannya; keputusan

analisis belauan x-ray (XRD) ke atas GO, GO:^{131}I, CSAC and CSAC:^{131}I menunjukkan nilai 2-theta (°) tertinggi pada 11.8°, 31.7°, 24.68° and 28.28°. Jarak-d (Å) dan indeks kehabluran (%) bagi setiap bahan juga diperoleh; spektroskopi x-ray fotoelektron (XPS) digunakan untuk mengkaji komposisi sesuatu bahan dan mendapati beberapa tenaga pengikat iaitu 283.95, 284.27, 285.29 and 287.10 eV merujuk kepada ikatan C-C, C=C, C-O, dan C=O pada spektra C1s. Spektrofotometri UV-Vis menganalisis kadar serapan bagi GO, GO:^{131}I, CSAC, dan CSAC:^{131}I; menunjukkan nilai 230, 210, 205, dan 223 nm yang didominasi oleh peralihan π-π* pada ikatan aromatik C-C. Berdasarkan keputusan dan mengambil kira ciri-ciri unik GO dan CSAC, kedua-dua bahan ini dibuktikan mampu menjadi kaedah alternatif bagi isolasi sisa kumbahan ^{131}I daripada tangki tangguh.

PERFORMANCE OF GRAPHENE OXIDE AND COCONUT SHELL ACTIVATED CARBON FOR ^{131}I ISOLATION FROM DELAY TANK

ABSTRACT

Iodine-131, with a half-life of 8 days and about 971 keV excess energy, is the well-known radionuclide used for hyperthyroidism and thyroid cancer. Due to its considered low-medium half-life, differentiated thyroid cancer (DTC) patients administered with high energy ^{131}I need to be isolated until at least minimal radiation exposure is achieved. An underground system known as a delay tank is used to withhold the ^{131}I and other clinical wastewater until a non-hazardous level is achieved and discharged into the main sewage system. The Nuclear Medicine Department, HUSM has only two isolation wards for the DTC patients and the delay tank of the department has a limited capacity hence linked to the restriction of patients' admissions. Thus, an alternative technique using graphene oxide (GO) and coconut shell activated carbon (CSAC) was proposed for isolating the ^{131}I clinical wastewater from the delay tank. The synthesized GO and CSAC were mixed with radioactive clinical wastewater with varying concentrations and filtered using membrane filter paper to collect the sediment. The decay rate of 5 mg/mL for both carbon-based materials was significantly higher than the concentrations 1, 2, 3, and 4 mg/mL, which indicates active interaction has occurred. The synthesized carbon-based materials, along with the sediments, were analyzed in several characterization studies; via Field Emission Scanning Electron Microscopy (FESEM), GO and CSAC were found appeared wrinkled-like tissue and had micropores on the surface, respectively; X-ray Diffraction (XRD) of GO, GO:^{131}I, CSAC and CSAC:^{131}I obtained 2-theta (°) peak values of 11.8°, 31.7°, 24.68° and 28.28° respectively that

are collateral with previous studies. The d-spacing (Å) and the crystallinity index (%) of each material were also obtained; X-ray Photoelectron Spectroscopy (XPS) was used for the composition study of the samples, which shows binding energy of 283.95, 284.27, 285.29 and 287.10 eV on C1s spectra that indicate the existence of C-C, C=C, C-O, C=O bonds respectively. The UV-Vis Spectrophotometry was used to analyze the sorption capability of GO, GO:^{131}I, CSAC, and CSAC:^{131}I; showing results of a 230, 210, 205, and 223 respectively, dominated by π-π* transition of aromatic C-C. Based on the results and underlining the unique features of both carbon-based materials, it is proven that these two materials can be used as an alternative method for the isolation of Iodine^{131} clinical wastewater from delay tanks.

CHAPTER 1

INTRODUCTION

1.1 Background of Study

Radioactive iodine (RAI) therapy is one of the nuclear medicine treatments for hyperthyroidism and differentiated thyroid cancer. RAI involves Iodine-131 (^{131}I), a beta-emitting radionuclide mainly accumulated in thyroid cells and targeted to treat only the thyroid gland. Based on Malaysia's summary of national cancer registry report of 2012-2016, thyroid cancer has taken up 8th place of cancer type in Malaysia with proportion of 1 in every 100,000 people. It is seen an increase of 3.2 incidence rate (ASR), especially in female thyroid cancer patients in 2016 from previous years (MOH, 2019). ^{131}I is purposely used to eliminate any remaining cancerous thyroid tissue and treat residual or persistent disease which helps decelerate the recurrence rate proportionally increasing the survival rate. The radioactivity of radionuclide administered to the differentiated thyroid cancer patients ranges between 1.85 GBq and 7.0 GBq (Ma et al., 2013), which makes the patients are compulsory to be hospitalized until the external dose rate reduced to a non-hazardous level to avoid any radioactive contamination risk. Certificates of authorization based on the Radioactive Substance Act 1993 declare the maximum activity that can be disposed of during set periods is less than 1.2μCi (44.4MBq) before the radioactive waste is discharged into the normal sewage system (Driver & Packer, 2001; Ravichandran et al., 2011).

The waste excreted by the patients cannot be flushed along with other medical waste via the hospital drainage system due to the decay time of the ^{131}I that

took eight days of half-life. Due to that, the waste is stored away in the delay tank until the activity reduces to the safety level that has been stipulated. Like any other waste storage, the delay tank also has periodic clearance time. Each standard delay tank took about five months before clearance before the other tank was filled simultaneously. The operational guideline stated that the maximum limit of average radioactivity concentration per month to discharge is 22.2 MBq/m^3 for ^{131}I (Ravichandran et al., 2011). Due to this, other than the ward availability for the patients, the delay tank capacities at a time before flush also is a major concern in planning the patients' treatment time and schedule. The number of patients getting RAI therapy at the Nuclear Medicine Department, HUSM, has tremendously reduced since 2017 by 80% due to alignment with delay tank capability determined by the Atomic Energy Licensing Act 304 Regulations. It should be theoretically estimated to avoid any redundant amount of waste at a time.

An initiative shall be taken to enhance the delay tank performance to improve the number of patients treated at a time. Carbon-based materials such as graphene oxide (GO) and coconut shell activated carbon (CSAC) are two of the best adsorbents used in wastewater treatment. GO has numerous oxygen-functional groups has made it capable of agglomerate with the other functional group within the clinical wastewater. GO is also capable of adsorbing a large amount of waste because of its unique feature of a high surface that is contributed by large pore volume and nanolayers feature (Razab et al., 2020). CSACs have been proven to be a good adsorber due to their high capacity, mild conditions, and easy regeneration (Liu et al., 2017). The existing product such as Radiacwash is formulated to decontaminate a wide range of radioactive contamination including radioisotopes without affecting

the surfaces meanwhile these carbon-based materials are proven can meet both purposes of decontamination and adsorption capability (Razab et al., 2022)

Through the carried-out experiment and preparation of GO via the Hummers method and CSAC with KOH activation, both carbon-based materials applications for effective isolation of radionuclide, specifically ^{131}I, from clinical wastewater were studied. The kinetic adsorption and UV-Vis absorption spectrum of the samples, along with the morphology studies via FESEM, XRD, and XPS, were analyzed to summarize GO and CSAC performances in secluding radionuclides from aqueous solution. The mechanism of clinical wastewater along with ^{131}I by carbon-based materials also has been discussed and illustrated.

1.2 Problem Statement

The delay tank that functions as waste storage has a specific volume of radioactive waste that can be stored at a time until the radioactivity decline to a safe level that is 22.2 MBq/m^3 for ^{131}I for monthly average concentration (Ravichandran et al., 2011). According to IAE, 5,000 litres each of two delay tanks should suffice for two-bed isolation ward. However, the two-bed isolation ward at Nuclear Medicine Department, HUSM is equipped with two tanks with a capacity of 3,568 litres each which has caused a limitation for patients' admission. The limited capacity is due to its standard protocol for the total capacity of filling it and periodical clearance of once in every 5 months (refer Appendix D) before the content is flushed out. This period of clearance has caused the exposure rate increased as the week went with the number of patients admission increased as well. According to the regulation set by the Atomic Energy Licensing Act 304, the existing delay tank are not impotent

to hold up four patients admission every month. This has caused reduction about 80% of patients from 2016 to 2017.

These standards have raised challenges in achieving effective and economical methods for the management of wastewater clearance. Furthermore, the ^{131}I which has a half-life of eight days, along with other clinical wastewater, need to be stored in the delay tank before being discharged into the ordinary sewage system (Mumtaz et al., 2009). This has subsequently limited the number of patient admission which indirectly lead to delays in patients' treatment schedule (Razab et al., 2020).

I hope this research can contribute to managing the decontamination procedure and enhance the decay rate of radioactive clinical wastewater in the delay tank. These findings of low-cost activated carbon are able to be used for the adsorption of contamination areas by substituting and improvising existing decontamination agents in the management of radioactive waste. This concentrated and contained method of transfiguring or agglomerating the radioactive wastewater into a solid form is believed to reduce the concentration activity and boost the radioactive waste clearance process.

1.3 Study Objectives

1.3.1 General Objectives

To propose an ^{131}I isolation method using carbon-based materials for alternative nuclear waste management

1.3.2 Specific Objectives

i. To synthesis and characterize graphene oxide and coconut shell activated carbon.

ii. To determine the kinetic radioactivity of clinical wastewater after isolation using graphene oxide and coconut shell activated carbon.

iii. To characterize the extraction product of radioactive clinical wastewater using FESEM, UV-VIS, XRD and XPS.

iv. To evaluate the adsorption mechanism of carbon-based materials towards radioactive clinical wastewater.

1.4 Study Significant

By conducting this study, the capabilities of carbon-based materials, GO and CSAC, as adsorbents for radioactive clinical wastewater specifically ^{131}I wastewater in nuclear medicine can be determined and proved. Hence, the synthesized GO and CSAC are able to redound to the benefit of radiation protection and safety, not only towards the research fields but also can be executed in the industry according to the application suitability.

Furthermore, the super adsorbing features of carbon-based materials can be used as an alternative method to clear the delay tank optimally in order to overcome the number of patients' admission restrictions that is increasing each day. Other than that, the GO and CSAC can probably be produced as a sponge or filter and acts as a decontamination agent. This is considered to be an entrepreneurship value and has the potential to be marketed. The innovative GO/CSAC sponge or filter can probably replace the less functioning existing decontamination agent such as Radiacwash.

1.5 Conceptual Framework

As in Figure 1.1, the conceptual framework has provided an overview of the research including the synthesis of carbon-based materials, varying the variables, analysis, characterization, and mechanism.

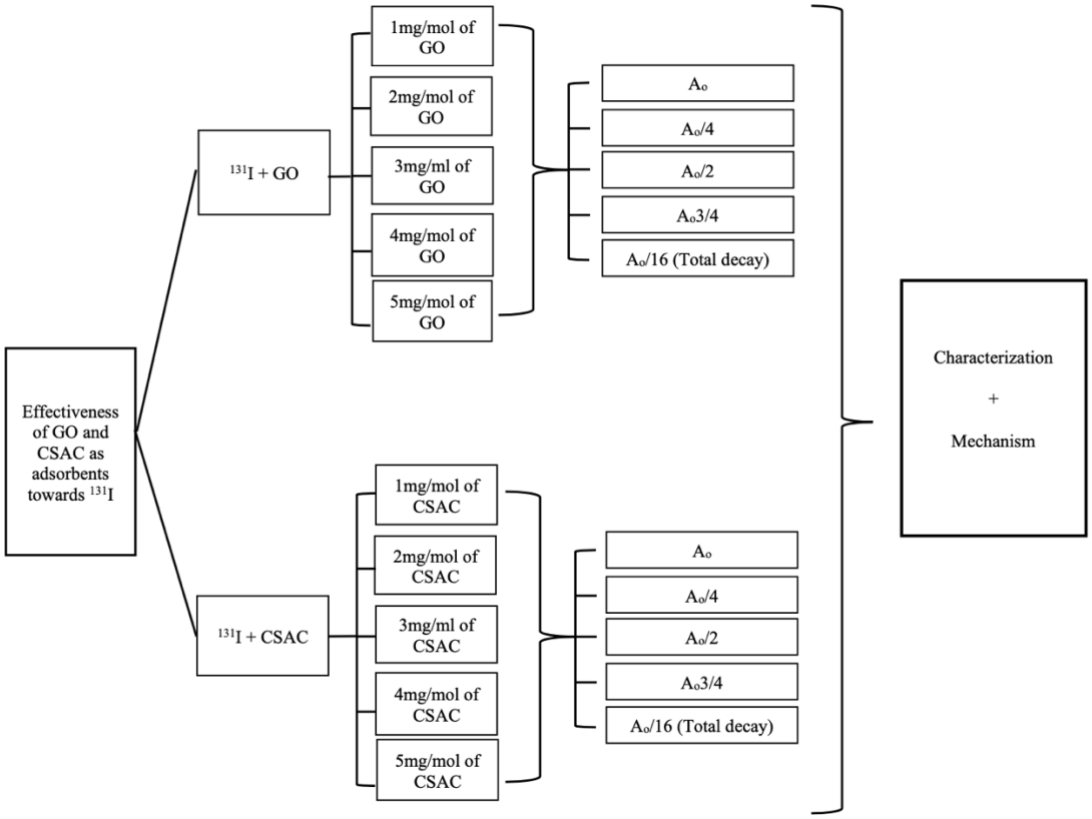

Figure 1.1 Conceptual framework of this research

CHAPTER 2

LITERATURE REVIEW

2.1 Radioiodine Therapy

Radioiodine or RAI therapy is a common treatment to treat hyperthyroidism and differentiated thyroid cancer by destroying hyperfunctioning and residual thyroid tissue. RAI gives out permanent destruction results towards the targeted thyroid tissue by emitting radiation of two types, gamma and beta rays. It is recommended for the patients with high surgical risk and short life expectancy or patients with intolerable oral antithyroid agents (Bahn et al., 2011). There are two main purposes of RAI therapy which are differentiated thyroid cancer (DTC) and Benign thyroid cancer (BTC), which have a dose range of >1110 MBq and 1110 MBq to 3700 MBq respectively (Buscombe et al., 2008). Due to the high activity in MBq in the DCT procedure, the patient is required to be hospitalized and restricted to close contact with anyone. The patient's activity reading need to be monitored until it becomes less than 1221 MBq (Pacini et al., 2016).

In nuclear medicine, both diagnostic imaging and radionuclide therapy essentially use radiopharmaceutical (RPC) as it plays a crucial role in diagnosing organs and treating pathological conditions, especially cancer or malfunctioning system (Payolla et al., 2019). The radioactive materials or RPCs are synthesised either in gasses, liquids, or solid materials, which are then administered to the patient through intravenous injection, orally, or inhaled radioactive gas or aerosol (Mattsson & Bernhardsson, 2013). RPCs have the capability to shrink tumours and kill

cancerous cells with a high intensity of the bombarding particles flow with adequate energy (Biricová & Kuruc, 2007).

RAI is an alternative treatment of choice other than surgery due to a ^{131}I half-life of just over eight days and targeted to treat only the thyroid gland (Mumtaz et al., 2009). The patient will orally ingest the iodine which will be rapidly absorbed in the form of iodide through the intestine and distributed in the blood pool as shown in Figure 2.1. Within three hours, it will reach its maximum level; once it reaches the thyroid gland, the iodide will be trapped in the blood pool. Iodide uptake by thyrocytes is mediated by sodium iodide symporter (NIS) located at the basal membrane before travelling to the apical membrane and then into the follicular lumen . The iodide then oxidized to iodide by peroxidase (Chudgar & Shah, 2017; Oh & Ahn, 2012). Iodothyronines are produced from the iodination of tyrosine residues present within the thyroglobulin molecules. Coupling the iodothyronines with thyroid peroxidase forms either triiodothyronine (T3) or thyroxine (T4). The iodine, as the natural precursor for thyroid hormones (T3 & T4), stays in the thyroid follicular cell by the sodium and NIS until it is released into circulation (Chudgar & Shah, 2017; Oh & Ahn, 2012). The thyroid gland has a high affinity for iodide and concentrates it to a level 20-40 times than the serum iodide levels.

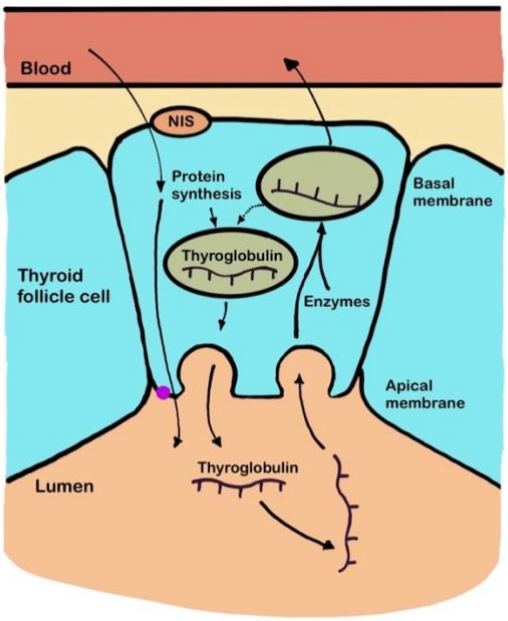

Figure 2.1 The ^{131}I uptake mechanism by the thyroid gland (Oh & Ahn, 2012)

Besides the thyroid gland, the iodine also accumulates at salivary gland, gastric mucosa, thymus, nose, oesophagus, colon and liver or any organs that expressing NIS. The kidneys will excrete up to 90% of the administered dosage, and only a small fraction is excreted in faeces and sweat (Chudgar & Shah, 2017). Urinary excretion is almost 50% in 24 hours after administration.

2.1.1 Decay Rate of ^{131}I Radionuclide

Radioactive decay refers to the loss of elementary particles from an unstable nucleus, forming another stable element (Mettler & Guiberteau, 2012). There are five types of radioactive decay which are alpha emission, beta emission, positron emission, electron capture, and gamma emission . As for ^{131}I, it is a beta and high energy gamma emitter with a half-life of 8 days before forming into a stable ^{131}Xe (Mody et al., 2015) and emits 364 keV of gamma energy simultaneously which can be seen in a simplified illustration in Figure 2.2. The decay rate is proportional to the number of atoms and the activity measured in terms of atoms per unit of time as in Equation 1, and it is

independent of the element's physical state such as the temperature and pressure surrounding ;

$$A = \lambda N \qquad \text{(Eq 1)}$$

Where A is the total activity and is the number of decays per unit time of a radioactive sample, N is the total number of particles in the sample and λ is the constant of proportionally or decay constant. It is important to take note that the decay constant of the radionuclide will remain unchanged in whatever process it may involve; however, the decay rate of the radioactive can be enhanced by some chemical reaction at the molecular level (Razab et al., 2022).

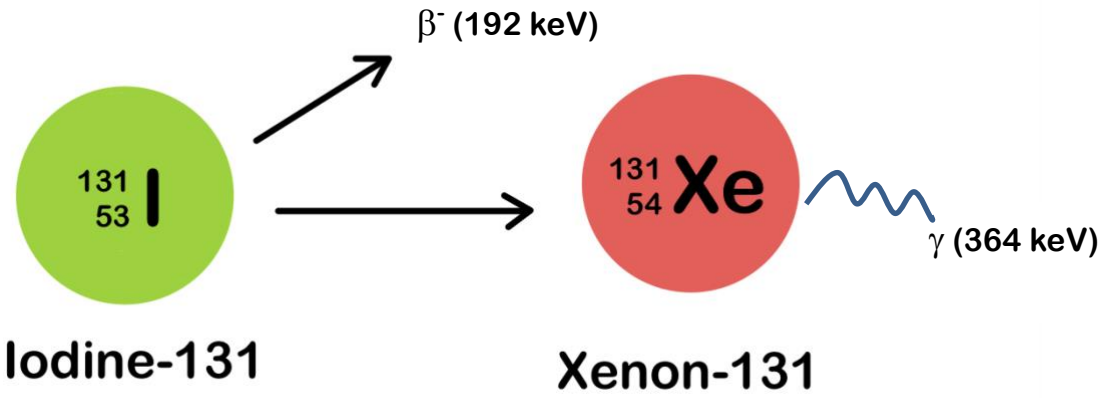

Figure 2.2 The radioactive decay of ^{131}I via betta emission obtaining a stable ^{131}Xenon and gamma radiation.

The main radionuclide used at Nuclear Medicine Department, HUSM are ^{99m}Tc and ^{131}I. Even though both radionuclide are taken up by the thyroid, ^{99m}Tc, a pure gamma emitter has much shorter half-life of 6.04 hours. Hence, ^{99m}Tc waste has a

shorter decay period which subsequently has a lower potential of exposure build-up than ^{131}I in the delay tanks.

2.2 Clinical Radioactive Waste Management and Delay Tank

Radioactive waste in healthcare contains radioactive substances including unused liquid from nuclear medicine uses or radiotherapy, contaminated glass, packages or absorbent paper, urine and excretion from treated with unsealed radionuclides patient also sealed sources (Kafle, 2015). Systematic and good management of radioactive clinical waste disposal in nuclear medicine has always been a concern for both health institutions and regulatory authorities. The important issues are safe custody of the received radioisotopes, surveillance for their safe applications in the department, and the disposal of the radioactive wastes generated from human use of these radioisotopes (Ravichandran et al., 2011). The monitoring of radiation activity is crucial in order to fulfil the two main aims of the regulatory system. First, to prevent the occurrence of deterministic effects in individuals by keeping doses below the relevant threshold. Second, to ensure that all reasonable steps are taken to reduce the occurrence of stochastic effects in the population.

The disposal of the radioactive waste generated from radioisotopes that have been administered to humans has been one of the issues in obtaining clearance from national regulatory authorities (Ravichandran et al., 2011). The radioactive waste disposals must be obliged according to the public safety limit of 1 mSv per year as recommended by the BSS Regulations. This close monitoring of radioactive waste disposals ensures that the degree of predicted dilution is achieved at the discharge point and protects the public member from significant radioactive hazards. The

radioactive waste can be managed either by storing the waste safely in a specific radioactive waste container until radioactive decay reduces the activity to a safe level or disposal of low-activity waste into the sewage system.

As for RAI patients, they will be hospitalized for at least 72 hours after the ^{131}I ingestion to allow biological elimination and attain an exposure rate of less than 10μSv/h at a distance of 1 m (Yusof et al., 2016). The outlets of the toilets and bathrooms of the patients undergoing the diagnostic and therapeutic procedures either with ^{99m}Tc or ^{131}I, are connected to the delay tank. A delay tank is an underground system to contain radioactive waste until certain radioactivity before discharging it into the main sewage system (International Atomic Energy Agency, 2013).

Based on a study by Yusof et al.,. (2016) on the public exposure in a radioiodine ward delay tank facility of Radiotherapy, Oncology and Nuclear Medicine, Department, HUSM, it is found that the exposure rate increased as the week went by as the number of RAI patient admitted risen as well. The findings also indicate that the delay tank facility gave a significant amount of public exposure despite its confinement in the delay tank facility. Figure 2.3 shows the floor plan of the measurement points from the delay tank room, where;

A: Inside the delay tank room at a 1 m distance from the delay tank

B: The door of the delay tank room

C: The public walking route in from of the delay tank room

D: The public walking route lateral to the delay tank room

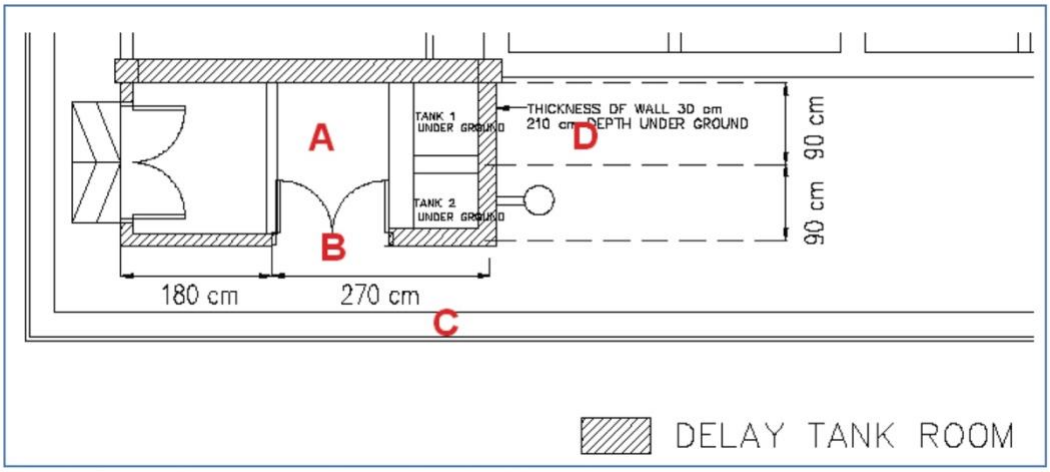

Figure 2.3 The plan of a measurement point at the ^{131}I delay tank room at the Nuclear Medicine department, HUSM (Yusof et al., 2016)

Based on the previous studies and the main concern regarding radioactive waste, it is crucial to find a way where the authorities can alternate or discharge the waste more efficiently to avoid any unnecessary exposure not only to the public, but also to the personnel. By conducting this study, the capability of the carbon-based materials as adsorbent towards the ^{131}I clinical wastewater can be proved and directly enhance the decay rate of the radionuclide involved in the delay tank facility.

2.2.1 Radioiodine Therapy and Delay Tank Operation at Nuclear Medicine Department, HUSM

Since 2015, the number of patients on radioiodine therapy (high dose) has been documented. It can be seen the first two years, 2015 and 2016, the number of patients exceeded 50 people and greatly reduced by about 80% to 36 patients in 2017. The number has been consistent for five constituent years; the highest number of patients is only 45. Unlike diagnostic scan purposes, which documented the record from 2018 to 2021, the number was tremendous for the past 4 years and reached 758 patients in 2021. The delay tank clearance can be seen in Appendix D.

This reduction in radioiodine therapy since 2017 is due to the existing delay tanks are not capable of holding four patients' admissions per month which need to meet the Atomic Energy Licensing Act 304 (Radioactive Waste Management) Regulations 2011. From the bar graph in Figure 2.4, it can be concluded the number of patients required to undergo radioiodine therapy may be high; however, it needs to be reduced due to the delay tank system capacity. This limitation has directly caused the number of people supposedly receiving such treatment to decrease and possibly affect their health.

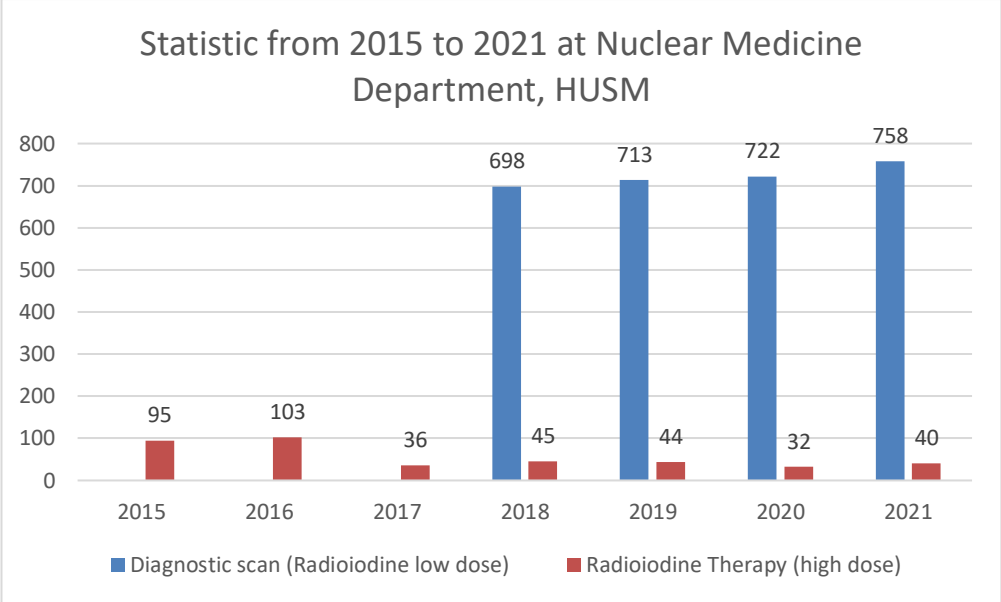

Figure 2.4 Bar chart represents the number of patients for each radioiodine therapy and diagnostic scan

2.2.2 Radiation Protection Principles in Malaysia

Basic radiation protection framework includes social and scientific considerations in providing for radiation protection without compromising gains and benefit from radiation exposure. The objectives of radiation protection concerns on preventing the occurrence of deterministic effect by restricting dose below thresholds and reducing induction of stochastic effects.

An agency named Atomic Energy Licensing Board (AELB) was formed to ensure the safe use of nuclear technology in medical and industries in Malaysia and under supervision of Malaysia's Ministry of Science, Technology and Innovation (MOSTI). AELB had been given the authority to implement the Act 304 1984. The AELB also provides training for radiation personnel, license for facilities involving the ionizing radiation, and also publications regarding the safe use of ionizing radiation. System of Radiation Protection is the name given by the International Commission on Radiation Protection (ICRP) to the application of three basic principles in Radiation Protection that are (1) justification of practice, (2) optimization of protection and safety, and (3) application on individual dose limit.

According to Atomic Energy Licensing Act (Act 304), all exposures of workers incurred in the course of their work, with the exception of exposures excluded from the standard and exposures from practices or sources exempted by the standards. The effective dose limit for whole body radiation of occupational personnel is 20 mSv per calendar year with additional restriction applies to the occupational exposure of pregnant woman which is 1 mSv for the remaining period of pregnancy. The Basic Safety Radiation Protection Regulations 2010 recommended the dose limits allowed for member of the public as 1 mSv per year. Dose limit in special circumstances or planned special exposure refers to voluntary exposure during normal operation whereby one or more of the annual dose limits for a worker is likely to be exceeded. Planned special exposure shall only be carried out when approved by the appropriate authorities that are AELB and Ministry of Health of Malaysia (MOH).

Protection against Occupational radiation hazard has been highlighted in Act 304 through classification of the working areas as in Table 2.1 (Yusof et al., 2016).

The classification of areas take into account of the likehood and magnitude of potential exposure risk also the nature and extent of the required protection and safety procedure. Area is demarcated with radiation warning signs and legible notices clearly posted. No person shall enter a controlled area unless he has been assigned to the area or has been authorized to enter the area.

Table 2.1 Classification of working areas

Work Areas	**Classification**
Clean	-Work area where the annual dose received by a worker is not likely to exceed the dose limit for a member of the public -Not involving application and usage of unsealed radionuclides
Supervised	-Work area for which the occupational exposure conditions are kept under review even though specific protective measures and safety provisions are not normally needed -Surface contamination: 2-7 $Bqcm^2$ -Contamination of suspended particle: 0.3-1 x 10^2 Bqm^3
Controlled area	Work area where specific protection measures and safety provisions could be required for controlling normal exposures or preventing the spread of contamination during normal working condition and preventing or limiting the extent of potential exposures annual dose to a worker is likely to exceed 3/10 ADL Surface contamination: >7 $Bqcm^2$ Contamination of suspended particle: >1 x 102 Bqm^3

2.3 Carbon-Based Materials

2.3.1 Graphene Oxide

Graphene oxide was derived from graphene, a two-dimensional material that can be obtained from graphite. The naturally occurring chemical structure of graphene comprised sp^2 hybridized bonded carbon atoms that interestingly appeared as a honeycomb structure (Abu-Nada et al., 2021; Alkhouzaam et al., 2020). GO has been the adsorbent material of choice rather than other technologies such as membrane filtration and ion exchange which can be costly and produce unnecessary discharge than be harmful to the environment (Abu-Nada et al., 2021). There is a number of research on the interestingly developed graphene-based adsorbents in removing heavy metals, which can lead to inauspicious effects on health and the environment. The founding of various developed GO was summarized in Table 2.2.

Table 2.2 Applications of GO as an adsorbent of heavy metals in wastewater

Year	Author	Findings
2013	Wang	-Removal of zinc from aqueous solution via GO and reported a maximum capacity of 246 mg/g
2017	Shahzad et al.	-EDTA-functionated chitosan-GO nanocomposite used Adsorb Pb, Cu, arsenic from water and achieved adsorption capacities
2017	Raghubanshi et al.	-Removal of lead ions from aqueous solution via GO and reported a maximum capacity of 120 mg/g
2020	Abu Nada	-EDTA-functionated chitosan-GO nanocomposite used Adsorb Pb, Cu, arsenic from water and achieved adsorption capacities
2021	Suksompong et al.	-Synthesized GO/CS sponges as an adsorbent for the removal of Iodine-131 from aqueous solutions
2022	Razab et al.	-GO was used as an alternative RPC spillage decontaminant for Fluorine-18: FDG in the PET scan

Besides being more environmentally friendly and economical, GO is known for its high surface area, high chemical stability, large pore volume structure, and abundant oxygen-containing functional group (Razab et al., 2020). The oxidation process resulted in numerous oxygen-containing functional groups at the extremity of GO nanolayers sheets resulting in hydrophilicity making it easier to be modify than the graphene-based materials (Alkhouzaam et al., 2020; Sitko et al., 2013).

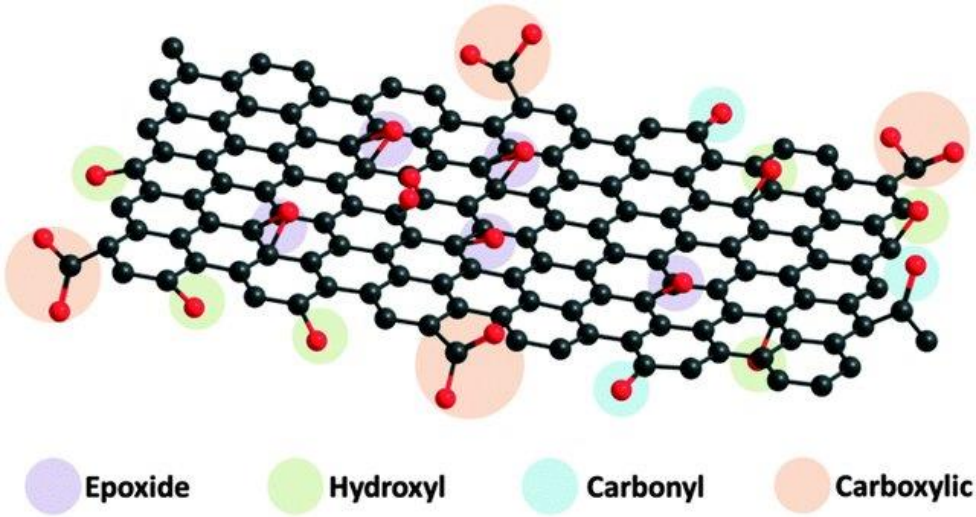

Figure 2.5 Graphene oxide honey-comb structure with various oxygen-containing functional groups (Ann Liebert et al., 1997)

The carboxylic groups are mainly located at the edges of the GO; meanwhile, hydroxyl and epoxy groups are attached to the basal plane of the GO, as depicted in Figure 2.5. Due to the abundant oxygen-containing functional groups, GO nanosheets become polar in nature and exfoliate easily in water-based solutions (Boehm, 1994). Adsorption of GO towards heavy metals can be described as physical absorption, chemical absorption, and electrostatic attraction. Chemical absorption and electrostatic attraction are two important components that influence the adsorption capability of GO.

Oxygen-contained functional groups have lone electron pairs and can bind efficiently to a metal ion to form a metal complex by sharing an electron pair. Other than that, the high surface area of GO is another factor for its high adsorption capacity. Not only is the GO is highly adsorptive towards heavy ion metals, but it is also proven capable in agglomerate radionuclide, both from pure RPC and wastewater (Razab et al., 2022; Suksompong et al., 2021). GO also claimed to be one of the highest capability carbon-based materials compared to any currently reported sorbents, including modified carbon nanotubes (Sitko et al., 2012).

Brodie's method was the first known GO synthesis method in 1859 which introduced the outstanding properties of graphene more than 150 years ago (Alkhouzaam et al., 2020; Feicht et al., 2019). Nitric acid and potassium chlorate OR sodium chlorate was mixed with graphite. This method has some drawbacks, including the time-consuming process that took about four days to complete the four required oxidation cycles of washing and drying (Alkhouzaam et al., 2020). This method is also very prone to a spontaneous explosion of chlorine dioxide gas (ClO_2), which results from the reaction between chlorate and acids (Alkhouzaam et al., 2020; Feicht et al., 2019; Muzyka et al., 2017; Zaaba et al., 2017). In 1958, Willian S. Hummers and Richard E. Offeman created the well-known Hummers method by using Sulfuric acid and sodium nitrate and potassium permanganate to oxidize graphite which has brought a much less time-consuming method and less hazardous due to the elimination of ClO_2. However, due to the usage of $NaNO_3$, the formation of toxic gas such as NO_2 and N_2O_2.

Modifications to Hummer's method have been made to get the most ideal in terms of preparation and safety. GO was prepared with a mixture of H_2SO_4 and H_3PO_4 and the addition of $KMnO_4$ with no $NaNO_3$ (Mohamed Noor et al., 2018; Razab et al.,

2020). This method was claimed to have higher GO's oxidation and yield compared to the conventional Hummer's method plus able to avoid the formation of toxic gas.

2.3.2 Coconut Shell Activated Carbon

Activated carbon (AC) has been widely known as an adsorbent for numerous environmental applications, including water treatment where AC is used as an adsorbent of natural organic compounds (Achaw & Afrane, 2008; Heidarinejad et al., 2020; Kosheleva et al., 2019). Evidences from previous studies shows that AC is prime industrial material due to its well-developed pore structure and adsorption properties (Abdul Khalil et al., 2013). It is also interestingly found that AC is used in the hydrometallurgy industry for the extraction of metals like gold and in medicine where they are synthesized as antidotes due to their high surface area, highly porous structure and ease of preparation with various starting materials (Achaw & Afrane, 2008; Baby et al., 2019).

The intrinsic properties which are the pore structure and chemical composition of the precursor material specified the application of the synthesized AC. The porosity is defined as the distance between the walls for slit-shaped pores or the radius for cylindrical pores and also acts as the active site for the adsorption process (Bernard E et al., 2013; Daud & Ali, 2004). There are three categories of pores as in Figure 2.6; micropore (<2 nm), mesopore (2-50 nm), and macropore (>50 nm) (Everm & Butterworths, 1972). The features of the pores also the specific surface area of different types of carbon precursors link directly to adsorption capabilities in various applications (Carbon Bansal et al., 1990; Li et al., 2020).

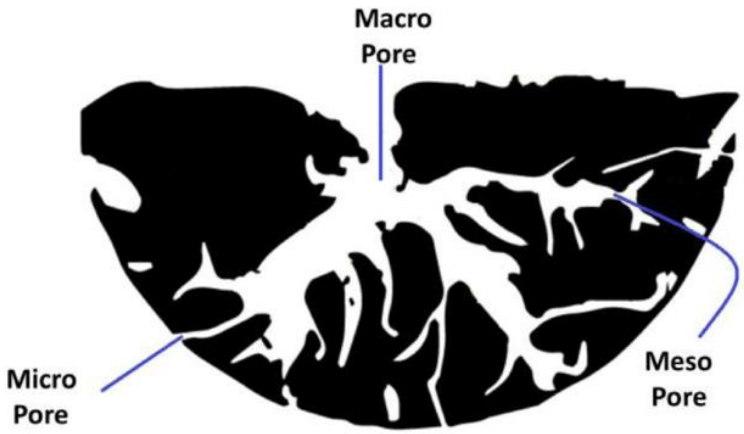

Figure 2.6 Different types of pores on activated carbon

In 1991, McDougall found that the coconut shell activated carbon has a fine pore distribution. Most of its pore volumes have less than 1 nm radius compared to wood based activated carbon, which has been observed to have significant amounts of mesopores and macropores. Other than that, it was also found that coconut shells had a high number of micropores and a smaller number of macropores which was vice versa compared to Miike coal (Dash et al., 1979). It is an important key feature to have a smaller average pore diameter because of the capability to adsorb nano pollutants. High microporosity means the rate of reaction can be higher due to the high availability of surface area (Daud & Ali, 2004). Table 2.3 has summarized the BET specific surface area (m^2/g) and average pore diameter (nm) based on various types of activated carbons.

Table 2.3 Comparison of BET specific surface area and average pore diameter from previous studies on different types of Activated Carbon

Year	Author	Type of activated carbon	BET specific surface area (m^2/g)	Average pore diameter (nm)
2018	Yang & Han	Coconut shell	1118.2	0.49
2021	Phothong et al.	Bamboo	907	1.025
2001	Hussein et al.	Oil palm trunk	1141	0.93
2020	Li et al.	Walnut shell	1545.3	>2.0
2011	Dolas et al.	Pistachio shell	1000	0.96

Material compositions such as lignin, cellulose and holocellulose are important parameters influencing the pore structure and distribution. In a study by Daud W. and Ali W. in 2004, they found that coconut shell has 19.8%, 68.7%, and 30.1% compared to palm shell, which consists of 29.7%, 47.7%, and 53.4% of cellulose, holocellulose and lignin respectively. The coconut shell has lower lignin content but higher holocellulose content, and vice versa to the palm shell. Due to that, it is found that the coconut shell char's activation rate is almost five times higher than palm chars. It is also claimed that lignocellulosic biomass has been a sustainable material in producing energy and chemical feedstocks (Abdul Khalil et al., 2013). It is also claimed that CSAC has numerous functional groups including hydroxyl groups, carbonyl groups, ethers, alkanes, alkenes and aromatic groups as a proof of lignocellulose compositions (Kwasi Opoku et al., 2021).

Besides the type of raw material, the type of porosity and pore distribution are also influenced by the activation method. There are two general activation methods

which are physical activation, which involves heating at 800°C meanwhile chemical activation involves heating at much a lower temperature, 500°C (Laine, 1992). There are a few widely used activators in chemical activation, such as phosphoric acid, zinc chloride, potassium carbonate, sodium hydroxide, and potassium hydroxide. Potassium hydroxide (KOH) has been one of the activators of choice in low-cost AC production because it is able to yield AC with high surface area, fine pore size under the same conditions, low environmental pollution, less corrosiveness, and also lower cost (Chayid & Ahmed, 2015; Hui & Zaini, 2015; Zuo et al., 2016). It is proven in studies that activation with KOH has yielded an AC with a higher microporous structure than NaOH and also that high amount of KOH, more micropores will develop while decreasing the mesopore due to the characteristics of the KOH activator (Ahmed & Theydan, 2014; Wu et al., 2010).

In this study, coconut shell is selected as one of the carbon-based adsorbents due to its abundant biomass availability and easy access. It is also due to its mechanical strength, low attrition rate, and microporosity distribution. The coconut shell has been chemically activated with KOH to produce a larger surface area and create much more micropores in order to increase the adsorption capability.

2.4 Adsorption Mechanisms in Aqueous Solution

The adsorption term defines the process where molecules accumulate in the interfacial layer, and the term ‘adsorbate’ refers to the material in the adsorbed state (Da, 2001). The adsorption technique is one of the most widely preferred technologies and effectively used to remove contaminants from wastewater due to its easy functioning, environmentally friendly and low-cost (Kwasi Opoku et al., 2021; Xu & Wang, 2017). The underlying concept of adsorption is linked to the equilibrium relation between the quantity of the adsorbed material and the pressure or